Photoemission study of itinerant ferromagnet $Cr_{1-\delta}Te$

K. Shimada, T. Saitoh, H. Namatame,* and A. Fujimori
Department of Physics, University of Tokyo, Bunkyo-ku, Tokyo 113, Japan

S. Ishida
Department of Physics, Kagoshima University, Kagoshima 890, Japan

S. Asano
College of Arts and Sciences, University of Tokyo, Meguro-ku, Tokyo 153, Japan

M. Matoba and S. Anzai
Faculty of Science and Technology, Keio University, Hiyoshi, Yokohama 223, Japan

(Received 21 June 1995)

The electronic structures of the itinerant ferromagnets $Cr_{1-\delta}Te$ ($\delta=0.05$, 0.25, and 0.375) have been studied by photoemission spectroscopy. The valence-band spectra are compared with the density of states given by band-structure calculations. In spite of the itinerant nature of the d electrons, disagreement between the photoemission spectra and the band-structure calculations exists in the magnitude of the d-band exchange splitting and the spectral weight at the Fermi level and 2–4 eV below it: The occupied d band for $\delta=0.05$ is shifted away from the Fermi level; the observed spectral weight at the Fermi level is significantly suppressed compared with the band-structure calculations for $\delta=0.05$ and 0.375, where the nominal d-electron numbers are close to integers 4 and 3, respectively. Configuration-interaction cluster-model calculations have been made for $\delta=0.05$ and 0.375 to explain the spectral weight distribution in the high-binding-energy (2–4 eV) region in terms of electron-correlation effects. The d-d on-site Coulomb energy is estimated to be significant, $U\sim 2$ eV, and nearly equal to or smaller than the charge-transfer energy $\Delta\sim 2$–3 eV.

I. INTRODUCTION

Chromium tellurides $Cr_{1-\delta}Te$ with metal-deficient NiAs-type structures[1–3] are ferromagnets with metallic conductivity.[4,5] The compounds have been known for their various magnetic structures and thermodynamical properties coupled with ferromagnetism. These properties have been discussed both from ionic and itinerant models, but their electronic states have not been clearly understood yet.

The compounds have ordered vacancies at the chromium sites.[1–3] Metal-deficient and metal-full layers stack alternatively along the c axis. The concentration of the metal vacancies (δ) is an important parameter for the crystal structures and the magnetic properties of the compounds. The Curie temperatures 325–360 K and the lattice parameter ratio $c/a\sim 1.56$ are almost constant for $0<\delta<0.25$, but they are significantly lower for $\delta>0.25$ ($T_C\sim 167$–170 K, $c/a\sim 1.51$ for $\delta=0.333$).[6–9] The pressure derivative of the Curie temperature $dT_C/dp(<0)$ remains almost constant for $0<\delta<0.25$ but decreases in absolute value for $\delta>0.25$ associated with the changes in the T_C and the c/a ratio.[6–9] The studies of the exchange striction[9–11] and the magnetostriction[12] have also revealed that the lattice parameters are strongly affected by the interaction between the magnetic moments on the Cr atoms, and that between the magnetic moments and external magnetic field. The paramagnetic susceptibilities of the compounds obey a Curie-Weiss law,[1,13–27] giving effective magnetic moments of around $\sim 4\mu_B$. They are well explained by the ionic model assuming Te^{2-} and mixed-valence Cr, as shown in Fig. 1. The observed ordered magnetic moments derived from the saturation magnetization,[1,13–28] 1.7–$2.5\mu_B$, however, are much smaller than the effective moments and the ordered moments calculated using the ionic model. According to neutron-diffraction studies,[29–36] the small saturation magnetization is partly explained if we take the spin canting into account for $\delta=0.125$, 0.167, and 0.25.[29] The magnetic moment induced on the Cr ion for $\delta=0.25$ is close to an integral number of Bohr magnetons, suggesting the existence of mixed valence Cr.[29] However for $\delta=0.333$, the ordered magnetic moment 2.65–$2.70\mu_B$, deduced from the neutron diffraction, is smaller than that calculated using the ionic model, $3\mu_B$, suggesting the itinerant nature of the d electrons.[29,30]

Band-structure calculations have been done on CrTe ($\delta=0$), Cr_3Te_4 (0.25), and Cr_2Te_3 (0.333) by Dijkstra *et al.*[37] Their calculations have given ordered magnetic moments of $3.51\mu_B$, $3.32\mu_B$, and $3.03\mu_B$ for $\delta=0$, 0.25, and 0.333, respectively. The calculated magnetic moments on Cr take almost the same values of $\sim 3.3\mu_B$ for the different δ's. The Te atoms also have a magnetic moment through the strong hybridization with the Cr $3d$ states varying from $-0.3\mu_B$ ($\delta=0$) to $+0.3\mu_B$ ($\delta=0.333$).[37] Recently, Ishida and Asano[38] made detailed band-structure calculations for $Cr_{1-\delta}Te$ with $\delta=0$, 0.25, and 0.333. For $\delta=0$, Ishida and Asano[38] have given somewhat smaller ordered magnetic moments of 2.44–$3.10\mu_B$ than that of Dijkstra *et al.*,[37] $3.51\mu_B$, whereas, for ferromagnetic $\delta=0.25$ and 0.333, both calculations have given almost equal magnetic moments of 3.0–$3.3\mu_B$. The magnetic moments are found to be very

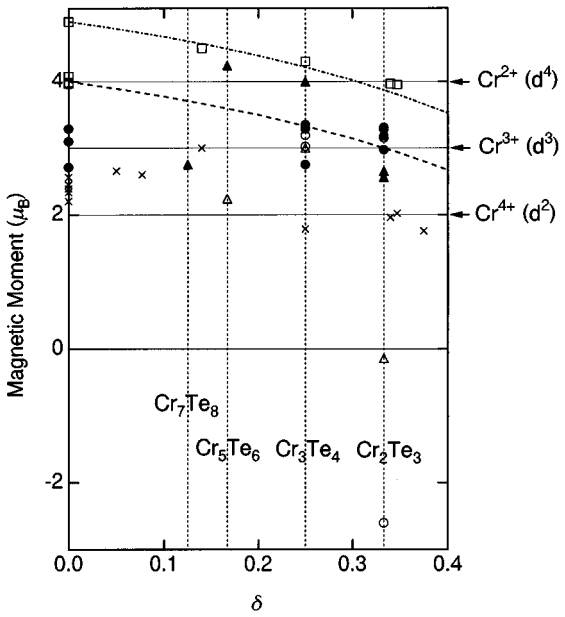

FIG. 1. Magnetic moments of $Cr_{1-\delta}Te$. The effective magnetic moments derived from the Curie-Weiss law (□) and the ordered moments determined by saturation magnetization (×) are taken from Refs. 1 and 13–28. The ordered magnetic moments in the metal-full layer (▲) and the metal-deficient layer (△) determined by neutron diffraction are taken from Refs. 29–32 and 36. The ordered moments for the metal-full layer (●) and the metal-deficient layer (○) given by band-structure calculations are taken from Refs. 37 and 38. The dot-dashed line (−●−) represents the effective moment in the ionic model, and the dashed line (- -) represents the ordered moment in the ionic model. The ordered moments for the high-spin d^4, d^3, and d^2 configurations in the ionic model are shown by arrows.

sensitive to the lattice parameters according to Ishida and Asano:[38] Only slight changes in the lattice parameters reduce the magnetic moment of $\delta=0$ toward the experimental value; in $\delta=0.333$ the magnetic moment of Cr in the metal-deficient layers easily changes its direction along the c axis as the volume of the unit cell changes. These facts partly explain the δ-dependent magnetic structures and magnetic moments of the compounds.

Grønvold and Westrum measured the heat capacities of $\delta=0.167$ (Cr_5Te_6), 0.25 (Cr_3Te_4), and 0.333 (Cr_2Te_3).[39] By fitting their experimental heat capacity (C) to the formula $C=\gamma T+AT^3$ below 18 K, we obtain the electronic specific-heat coefficients of $\gamma\sim 10$, 1, and 4 mJ/atom/K^2 for $\delta=0.167$, 0.25, and 0.333, respectively. These γ values show a minimum at $\delta=0.25$. The band-structure calculations[37,38] have given $\gamma\sim 1.0$–1.4 mJ/atom/K^2 for $\delta=0.25$ and $\gamma\sim 0.82$–0.96 mJ/atom/K^2 for $\delta=0.333$.[37,38] Thus the experimental γ value for $\delta=0.25$ is close to the calculated value, while those for $\delta=0.333$ and probably that for $\delta=0.167$ are considerably enhanced.

The optical reflectivity spectra of $\delta=0.25$ (Cr_3Te_4) and 0.333 (Cr_2Te_3) have been measured[40] and compared with the joint density of states calculated using the density of states (DOS) given by Dijkstra *et al.*[37] While agreement between the theoretical and experimental spectra for $\delta=0.25$ is good, that for $\delta=0.333$ is not satisfactory. It has been suggested that the poor agreement for $\delta=0.333$ may result from electron-correlation effects because the d electrons would have more localized character in $\delta=0.333$ than in $\delta=0.25$ due to the increased vacancy concentration.[40]

In order to obtain more direct information on the electronic states of these compounds, we have performed photoemission studies of $\delta=0.05$ ($Cr_{0.95}Te$), 0.25 (Cr_3Te_4), and 0.375 (Cr_5Te_8). Since this is a metallic system, first we consider the electronic states starting from the itinerant electron model, and we compare the valence-band spectrum with the DOS given by the band-structure calculations.[37,38] With the detailed comparison between observed spectra and the DOS's, we found that there exist disagreements. If the electron-correlation effect is important, the electrons tend to localize on the atom sites rather to extend all over the crystal, and the local-moment picture may be effective. In order to examine electron correlation, we have employed the configuration-interaction (CI) cluster model, which is a localized electron model but treats electron correlation effects correctly. As shown below, the calculation could explain the overall shape of the observed spectrum of $Cr_{0.95}Te$ and Cr_5Te_8 showing the importance of electron-correlation effects. We have estimated values for the parameters that characterize the electronic states of these compounds. The obtained parameters suggest strong p-d hybridization, which is consistent with the results of the band-structure calculation.

II. EXPERIMENT

Polycrystalline $Cr_{1-\delta}Te$ samples with $\delta=0.05$ ($Cr_{0.95}Te$), 0.25 (Cr_3Te_4), and 0.375 (Cr_5Te_8) have been prepared by the following procedures. To prepare $Cr_{0.95}Te$, a mixture of appropriate amounts of Cr and Te powders was sealed in an evacuated silica tube and gradually heated up to 600 °C for one week, kept at 800 °C for one day and at 1000 °C for one day. The product was crushed and fired gradually up to 1200 °C for 2 h, melted at 1330–1350 °C for 50 min, cooled down to 800 °C for 4 h and then quenched. Finally, the sample was heated up to 1000 °C, annealed for 5 h, and quenched into iced water. In order to avoid oxygen contamination from the silica tube, all the samples for $\delta=0.05$, 0.25, and 0.375 were melted in the silica tubes, whose inner walls were coated with amorphous carbon thermally decomposed from acetone. The silica tube was further enclosed in an outer one. Powder x-ray-diffraction pattern of $\delta=0.05$ showed a NiAs-type structure with lattice parameters of $a=4.018\pm0.002$ Å and $c=6.260\pm0.002$ Å. As for Cr_3Te_4, Cr, and Te powders sealed in an evacuated silica tube were slowly heated up to 700 °C, kept at that temperature for three days, and then cooled to room temperature. The product was crushed, slowly heated up to 1300 °C, and then melted. Powder x-ray diffraction indicated that the crystal structure was monoclinic with the lattice parameters $a_m=6.87$ Å ($=\sqrt{3}a$), $b_m=3.94$ Å ($=a$), $c_m=12.30$ Å ($=2c$), and $\beta=91.2°$. A mixture of Cr and Te powders for Cr_5Te_8 was slowly heated up to 850 °C for two weeks and kept at that temperature for four weeks. The products were transferred into the evacuated silica tubes, gradually heated up to 1240 °C for 6 h and melted. The sample was kept at this temperature for 50 min, and slowly cooled down to 800 °C for 3 h. It was homogenized at 800 °C for one week.

Then it was quenched into iced water. Powder x-ray diffraction showed that the crystal structure was of the CdI_2 type, with hexagonal lattice parameters $a=3.924\pm0.008$ Å and $c=6.008\pm0.010$ Å. The Cr vacancies are randomly arranged in the second basal planes of Cr atoms. The Curie temperatures of these compounds were $T_C=345$, 325, and 220 K, respectively.

Photoemission experiments were carried out using a spectrometer equipped with a Mg x-ray source (Mg $K\alpha$: $h\nu=1253.6$ eV) for x-ray photoemission spectroscopy (XPS) and a helium discharge lamp (He I: $h\nu=21.2$ eV) for ultraviolet photoemission spectroscopy (UPS). The total-energy resolution was ~1 eV for XPS and ~0.2 eV for UPS. The energy calibration has been done using the Cu $2p$ and Au $4f$ core-level photoemission spectra of Cu and Au metal, respectively, for XPS and using the Fermi edge of Au for UPS. UPS and XPS measurements of Cr_5Te_8 were made both at room temperature and liquid-nitrogen temperature (~80 K) in order to study the spectral change above and below the Curie temperature. XPS measurements of $Cr_{0.95}Te$ and Cr_3Te_4 were performed at room temperature, where they were in ferromagnetic states. The base pressure of the spectrometer was $\sim2\times10^{-10}$ Torr.

Photoemission measurements were also made at beamline BL-2 of Synchrotron Radiation Laboratory, Institute for Solid State Physics, University of Tokyo. The total resolution was 0.3–0.5-eV full width at half maximum (FWHM), depending on the incident photon energies $h\nu=41$–80 eV used in this work. The energy calibration was made using the Fermi edge of evaporated Au. The vacuum of the analyzer chamber during the measurements was better than 3×10^{-10} Torr. Measurements were performed at room temperature, where $Cr_{0.95}Te$ and Cr_3Te_4 were in the ferromagnetic states and Cr_5Te_8 was in the paramagnetic state. In order to obtain clean surfaces, the samples were scraped *in situ* with a diamond file. No oxygen $1s$ core-level peak or carbon $1s$ core-level peaks were detected by XPS, nor oxygen $2p$ emission in the valence band by UPS.

III. RESULTS

Figure 2 shows photoemission spectra of $Cr_{0.95}Te$ taken with photon energies of $h\nu=80$ and 1253.6 eV. At $h\nu=80$ eV, the atomic photoionization cross section of Cr $3d$ is ~50 times[41] as large as that of Te $5p$. At $h\nu=1253.6$ eV, on the other hand, the cross section of Te $5p$ is about two times as large as that of Cr $3d$.[41] Therefore, by comparing the two spectra, we can assign the peak at binding energy $E_B\sim1$ eV in the $h\nu=80$-eV spectrum to the Cr $3d$ band, and the peak at $E_B\sim2.5$ eV in the XPS spectrum to the Te $5p$ band. Valence-band spectra taken at $h\nu=80$ and 1253.6 eV for various δ's are shown in Fig. 3. As δ increases, the width of the Te $5p$ band decreases, which may reflect the narrowing of the band due to the increased vacancies. Compared with $\delta=0.05$, the Te $5s$ peaks of $\delta=0.25$ and 0.375 are slightly shifted toward the Fermi level, implying that the Fermi level is lowered with δ. The difference between $\delta=0.25$ and 0.375 is not clear in the valence-band spectra.

Figure 4 shows photoemission spectra of Cr_5Te_8 taken near the Cr $3p\rightarrow$Cr $3d$ photoabsorption threshold ($h\nu\sim42$ eV). Arrows in the figure show the Cr $M_{2,3}VV$ Auger peaks.

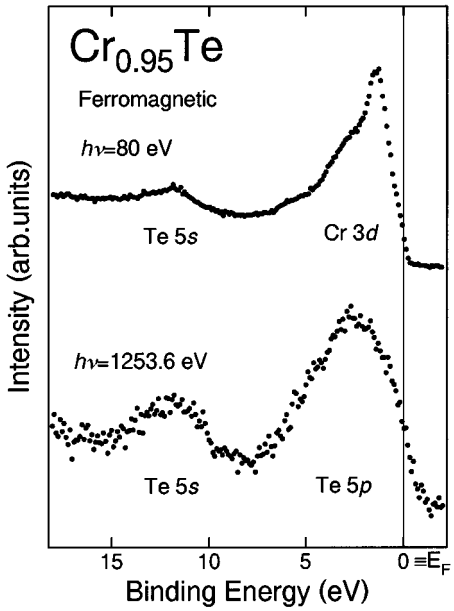

FIG. 2. Photoemission spectra of $Cr_{0.95}Te$ taken at $h\nu=80$ and 1253.6 eV.

The leading peak at $E_B\sim1$ eV is strongly enhanced around $h\nu=47$ eV. By subtracting the $h\nu=41$ eV (off-resonance) spectrum from the $h\nu=47$ eV (on-resonance) spectrum, we have obtained a resonantly enhanced Cr $3d$ component as shown in Fig. 4. Figure 5 shows the Cr $3d$-derived spectra of $Cr_{1-\delta}Te$ thus obtained for various δ's, and the corresponding $h\nu=80$-eV spectra. The overall features of the difference spectra agree well with those of the $h\nu=80$-eV spectra. Due to the non-negligible contributions from the Te $5p$ bands near the Fermi level at $h\nu=80$ eV, and to the difference in

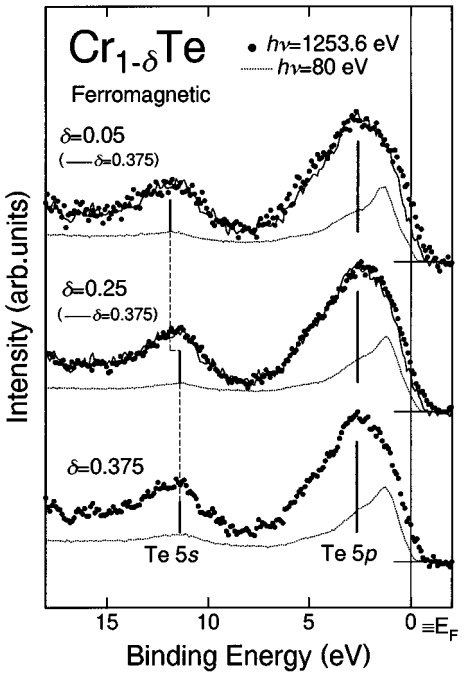

FIG. 3. Valence-band photoemission spectra of $Cr_{1-\delta}Te$ taken at $h\nu=1253.6$ and 80 eV.

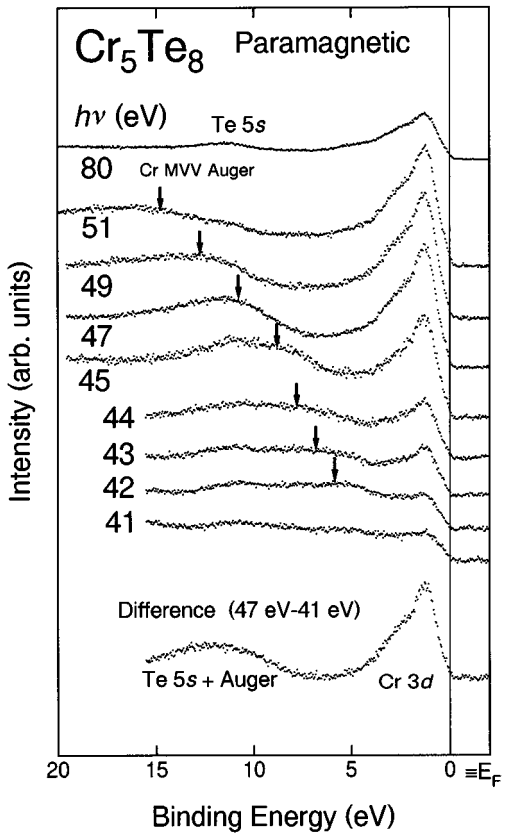

FIG. 4. Resonant photoemission spectra of Cr_5Te_8. The difference spectrum on the bottom has been obtained to deduce the Cr 3*d*-derived photoemission spectrum. Arrows show the Cr $M_{2,3}VV$ Auger peaks.

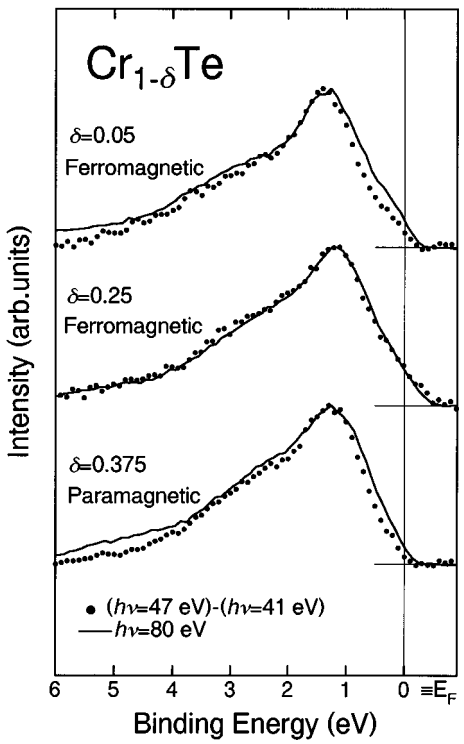

FIG. 5. Cr 3*d*-derived spectra obtained by resonant photoemission compared with the spectra taken at $h\nu = 80$ eV.

the energy resolution, the intensities of the $h\nu = 80$-eV spectra near E_F are a little higher than those of the difference spectra. The spectra show finite intensities at E_F, consistent with the metallic behavior of the compounds. The leading peak at $E_B \sim 1.2$–1.5 eV is accompanied by a broad shoulder extending from $E_B \sim 2$ eV to $E_B \sim 6$ eV. The width of the Cr 3*d* band in $Cr_{1-\delta}Te$ are found to be ~ 4 eV.

Overlapping Cr 2*p* and Te 3*d* core-level spectra are shown in Fig. 6. Since the binding energies of the Cr 2*p* and Te 3*d* core levels are very close to each other, it is difficult to decompose the spectra into the two components. Due to the large photoionization cross section of the Te 3*d* orbitals compared with the Cr 2*p* orbitals [Te 3*d*/Cr $2p = 2.6$ (Ref. 41)], the Te 3*d* component is dominant in these spectra. Figure 6 shows that the binding energies of the peaks move slightly toward lower binding energies with δ, consistent with the shifts of the Te 5*s* level (Fig. 3), and hence with the lowering of the Fermi level with δ.

Figure 7 shows the Cr 3*s* core-level spectra of $Cr_{0.95}Te$, Cr_3Te_4, and Cr_5Te_8. The Cr 3*s* spectra are superimposed on the tail of a plasmon satellite accompanying the Cr 3*p* peak located at around $E_B \sim 59$ eV. The Cr 3*s* spectrum of Cr_5Te_8 was measured both at room temperature and at liquid-nitrogen temperature, i.e., above and below the Curie temperature ($T_C = 220$ K). All 3*s* spectra show two peaks or an unusually broad peak which is consistent with two unresolved peaks, showing the existence of exchange splitting. The splitting reflects the magnetic moment of the Cr 3*d* valence electrons. If the *d* electrons are itinerant, the exchange interaction between the core hole and the spin-polarized Cr 3*d* band electrons will give rise to two peaks with equal intensities.[42] On the other hand, if the *d* electrons are localized, the two peaks have an intensity ratio of $I = S/(S+1)$, where *S* denotes the total spin of the localized Cr 3*d* electrons.[43] We have fitted the Cr 3*s* spectra assuming both

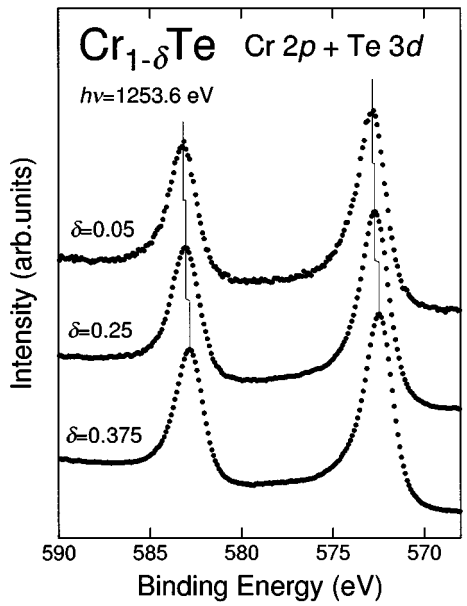

FIG. 6. Cr 2*p* and Te 3*d* core-level photoemission spectra of $Cr_{1-\delta}Te$ ($\delta = 0.05$, 0.25, and 0.375).

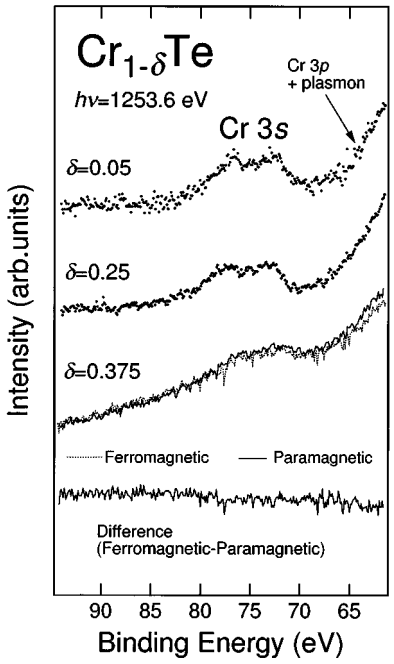

FIG. 7. Cr 3s core-level photoemission spectra of $Cr_{1-\delta}Te$ ($\delta=0.05$, 0.25, and 0.375). The difference spectrum between the ferromagnetic (dots) and paramagnetic (solid curve) state is also shown for $\delta=0.375$.

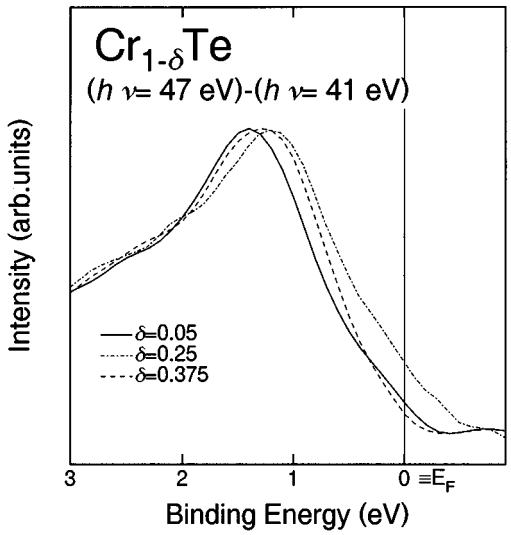

FIG. 8. Cr 3d-derived photoemission spectra near the Fermi level obtained by resonant photoemission. The data have been smoothed.

the above two models, and obtained equally good results because in the fitting procedure there was a large ambiguity in the background due to the overlapping plasmon tail. We need more detailed investigation to determine whether the exchange splitting is due to itinerant or localized Cr 3d electrons. The Cr 3s spectra of Cr_5Te_8 show only a small change above and below the Curie temperature, as shown in Fig. 7, indicating that the magnitude of the local Cr 3d magnetic moment remains essentially the same between the two phases. Little change was also observed for the valence-band spectra of Cr_5Te_8 above and below the Curie temperature, which is consistent with the Cr 3s spectra.

IV. ANALYSIS AND DISCUSSION

A. Electronic structure near the Fermi level

In order to clarify the changes of the spectra with δ, Fig. 8 shows smoothed Cr 3d-derived spectra near the Fermi level for various δ's. The intensities are normalized to the peak height. In going from $\delta=0.05$ to $\delta=0.25$, the main peak is slightly shifted toward the Fermi level, while in going from $\delta=0.25$ to $\delta=0.375$, it is shifted back toward higher binding energy. Consequently, the intensity at the Fermi level is the highest at $\delta=0.25$. If we assume the Te valence to be $2-$, the nominal d-electron numbers in $Cr_{0.95}Te$, Cr_3Te_4, and Cr_5Te_8 are ~ 4, 3.333, and 2.8 per Cr atom, respectively. Since the Cr ions are octahedrally surrounded by Te ions, the Cr 3d orbitals are split into threefold-degenerate t_{2g} levels and twofold-degenerate e_g levels. If we assume high-spin configurations for the Cr ions, the $t_{2g\uparrow}$ band is filled by three electrons, and additional electrons enter the $e_{g\uparrow}$ band as shown in Fig. 9. As δ increases from $\delta=0.05$ to $\delta=0.25$, the Fermi level moves downwards within the $e_{g\uparrow}$ band while the $t_{2g\uparrow}$ band remains almost filled. The $e_{g\uparrow}$ band in $Cr_{0.95}Te$ is nearly half-filled, and the system may be close to a Mott insulator. Therefore electron correlation would be strong in $Cr_{0.95}Te$. The $e_{g\uparrow}$ band is nearly empty in Cr_5Te_8, and the Fermi level lies in the region where the bottom of the $e_{g\uparrow}$ band and the top of $t_{2g\uparrow}$ band overlap. Again the system is close to a Mott insulator, and electron correlation is strong. On the other hand, the number of electrons in the $e_{g\uparrow}$ band in Cr_3Te_4 strongly deviates from an integer filling compared with $Cr_{0.95}Te$ and Cr_5Te_8, which would make the system a more ordinary d-band metal. Indeed, the intensity at the Fermi level is the highest for Cr_3Te_4, as shown in Fig. 8.

The above result corresponds well to the heat-capacity measurements,[39] where the electronic specific-heat coefficient γ is enhanced for $\delta=0.167$ (Cr_5Te_6) and $\delta=0.333$ (Cr_2Te_3), but not for $\delta=0.25$ (Cr_3Te_4): The specific-heat

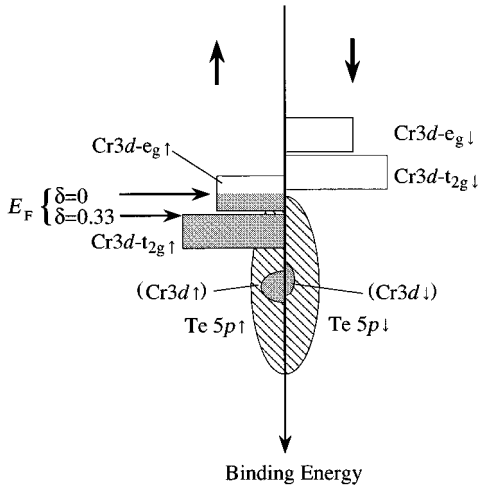

FIG. 9. Schematic view of the electronic structure of $Cr_{1-\delta}Te$. (Cr 3$d\uparrow,\downarrow$) denotes the Cr 3d component hybridized with the Te 5p band.

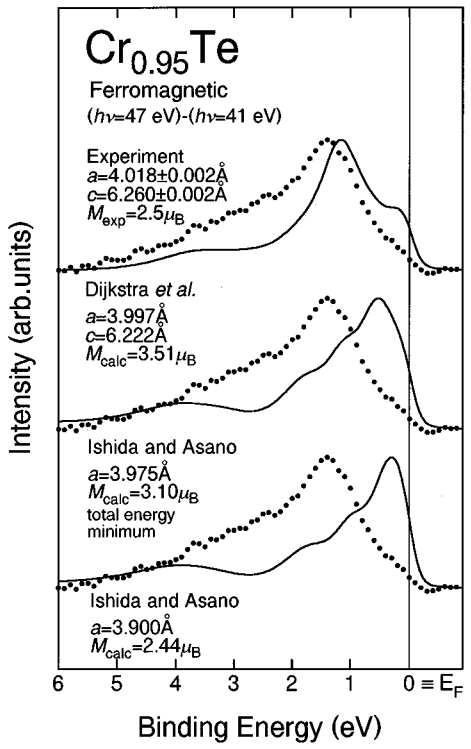

FIG. 10. Cr $3d$-derived photoemission spectrum of $Cr_{0.95}Te$ (dots) compared with the Cr $3d$ partial DOS of CrTe given by the band-structure calculations (solid curves) (Refs. 37 and 38). M_{expt} and M_{calc} are the experimental and calculated ordered magnetic moments, respectively. a and c with the theoretical DOS indicate the lattice parameters used in the band-structure calculations (Refs. 37 and 38). In the calculation of Ishida and Asano, the lattice-parameter ratio c/a is fixed at ~ 1.557.

results imply that correlation effects become significant as the band filling becomes close to an integer.

B. Comparison with band-structure calculations

We now compare the photoemission spectra with the DOS given by the band-structure calculations. Dijkstra *et al.*[37] performed band-structure calculations for $\delta=0$ (CrTe), 0.25 (Cr_3Te_4), and 0.333 (Cr_2Te_3) using the augmented-spherical-wave (ASW) method, whereas Ishida and Asano[38] used the linear muffin-tin orbital (LMTO) method. Both calculations took scalar relativistic effects into account. These two methods are quite similar, and are not expected to give large differences. Ishida and Asano,[38] however, optimized the radii of atomic spheres for Cr, Te, and vacancies, so as to give a total-energy minimum and to reproduce experimental lattice parameters. Spins are supposed to be collinear in both calculations. According to band-structure calculations, the Cr $3d$ partial DOS below the Fermi level consists of the $t_{2g\uparrow}$ band located at $E_B \sim 1$ eV, and the broad structure at around $E_B \sim 3$ eV which originates from Cr $3d$ character hybridized into the broad Te $5p$ band lying at $E_B = 2.5$–7.5 eV, as shown schematically in Fig. 9. Near the Fermi level there are also some contributions from the bottom of the Cr $3d$-$e_{g\uparrow}$ band, and from the Cr $3d$-$t_{2g\downarrow}$ band for $\delta=0$.

In Figs. 10–12, the experimental Cr $3d$-derived spectra of $Cr_{0.95}Te$, Cr_3Te_4, and Cr_5Te_8 are compared with the theoretical Cr $3d$ partial DOS's of CrTe, Cr_3Te_4, and Cr_2Te_3.[37,38] The ferromagnetic theoretical DOS is in reasonable agreement with the features in the experimental spectra, suggesting the itinerancy of the d electrons and the relevance of the band-structure calculations. As for Cr_3Te_4 and Cr_2Te_3, Ishida and Asano[38] made calculations for the ferrimagnetic state, where the metal-full and metal-deficient layers are antiferromagnetically coupled. As shown in Figs. 11 and 12, the peak position in the ferrimagnetic calculation is shifted towards the Fermi level compared with the ferromagnetic calculation. As for the peak positions, the ferromagnetic DOS is closer to the experimental spectra.

Here, in order to take into account the finite instrumental resolution and the lifetime broadening, the theoretical DOS has been broadened with Gaussians of 0.4- and 0.5-eV FWHM for $\delta=0.05$, 0.375, and $\delta=0.25$, respectively, and a Lorentzian whose FWHM (2Γ) increases linearly with binding energy E_B as $2\Gamma=0.2E_B$. Since no band-structure calculations are available for Cr_5Te_8, the ferromagnetic and paramagnetic DOS's of Cr_5Te_8 have been approximately synthesized out of the DOS's of Cr_2Te_3 and CrTe as follows. The Cr $3d$ and Te $5p$ partial DOS's of ferromagnetic Cr_2Te_3 were multiplied by $\frac{5}{2}$ and $\frac{8}{3}$, respectively, and the Fermi level was shifted so as to contain the appropriate number of electrons for Cr_5Te_8. As for the paramagnetic DOS for Cr_5Te_8, we have applied a similar procedure using the Cr $3d$ and Te $5p$ partial DOS's of the paramagnetic CrTe.

If we compare the DOS's given by the band-structure calculations and the photoemission spectra in more detail, some discrepancies can be identified. First, while the experimental Cr $3d$-$t_{2g\uparrow}$ peak positions in Cr_3Te_4 and Cr_5Te_8 agree well with those of the theoretical ones, as shown in Figs. 11 and 12, that in $Cr_{0.95}Te$ is shifted toward higher binding energy compared with the theoretical one, as shown in Fig. 10. It should be noted that the exchange energy in the band-structure calculation cannot be underestimated, since the calculated ordered magnetic moment is larger than the experimental one. As shown in Fig. 10, as the calculated magnetic moment and the exchange splitting of the Cr $3d$ band are reduced, the Cr $3d$-$t_{2g\uparrow}$ peak is shifted toward the Fermi level. That is, the calculated DOS of the Cr $3d$ band corresponding to the magnetic moment of $2.44\mu_B$, which is closest to the experimental value $2.5\mu_B$, is quite different from the photoemission spectrum. On the other hand, the DOS given by Dijkstra *et al.* is the closest to the photoemission spectrum in spite of the large discrepancy in the ordered magnetic moment. According to Ishida and Asano,[38] the peak position of the Cr $3d$-$t_{2g\uparrow}$ band in the calculated band structure of CrTe is not significantly dependent on the choice of the exchange-correlation potential. Therefore it is difficult to shift the Cr $3d$-$t_{2g\uparrow}$ band in CrTe toward higher binding energy as long as one assumes a collinear spin structure. As described in Sec. I, the small observed saturation magnetization for $\delta=0.125$ (Cr_7Te_8), 0.167 (Cr_5Te_6), and 0.25 (Cr_3Te_4) is explained within the ionic model if the spin canting is taken into account, as suggested by neutron-diffraction studies.[29,31,32,36] As for CrTe, although the magnetic structure has not been unambiguously determined so far, antiferromagnetic reflections coexist with the ferromagnetic ones in the neutron diffraction,[33–35] suggesting a spin canting. If the reduced saturation magnetization of CrTe is

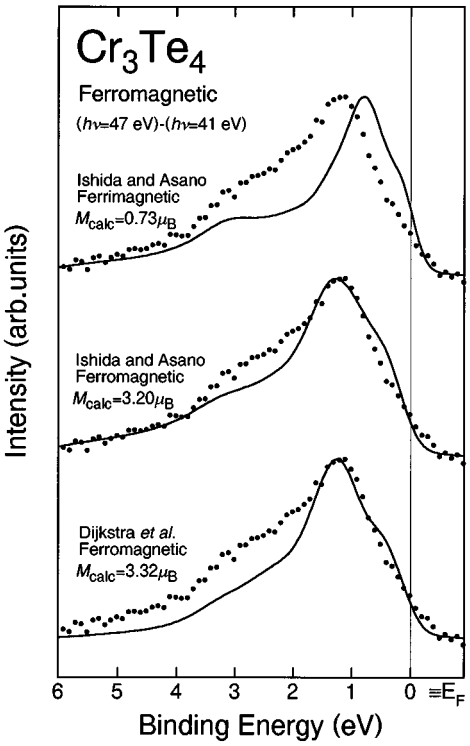

FIG. 11. Cr $3d$-derived photoemission spectrum of Cr_3Te_4 (dots) compared with the Cr $3d$ partial DOS given by the band-structure calculations (solid curves) (Refs. 37 and 38). M_{calc} is the calculated ordered magnetic moment (Refs. 37 and 38).

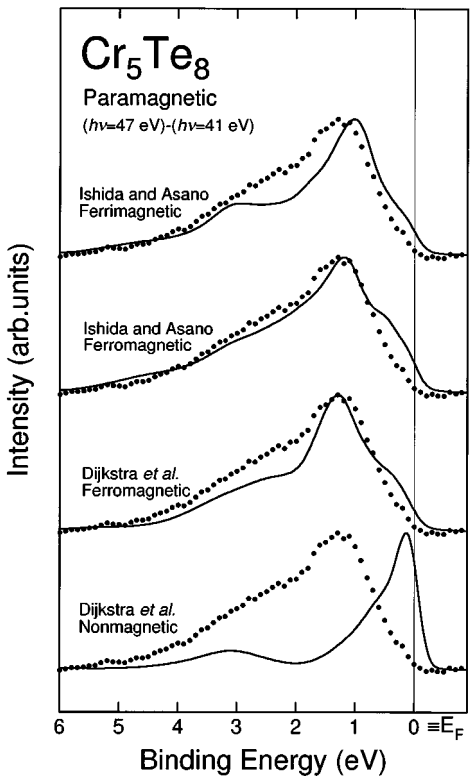

FIG. 12. Cr $3d$-derived photoemission spectrum of Cr_5Te_8 (dots) compared with the Cr $3d$ partial DOS given by the band-structure calculations (solid curves) (Refs. 37 and 38).

due to a spin-canting effect, band-structure calculations with canted spin structure would clarify the origin of the discrepancies between the photoemission spectra and the band-structure calculations.

Another discrepancy between the photoemission spectra and the band-structure calculations is that the photoemission intensity at the Fermi level is smaller than the theoretical DOS, particularly for $\delta=0.05$ and 0.375. As for $\delta=0.25$, the photoemission intensity at the Fermi level is highest among these compounds, and agrees well with the calculated DOS. This suggests that band theory is most appropriate for $\delta=0.25$, and that the low photoemission intensities at the Fermi level in $\delta=0.05$ and 0.375 compared to the calculated DOS are due to effects of electron correlation.

The intensity at $E_B \cong 2-4$ eV is stronger than the theoretical DOS, particularly for $\delta=0.05$. The intensity of this portion of the photoemission spectra is not so much dependent on δ. In the Cr $3d$ partial theoretical DOS, this part originates from hybridization between the Cr $3d$ and Te $5p$ bands. The discrepancy may indicate that hybridization between the Cr $3d$ and Te $5p$ bands as observed by photoemission is stronger than that predicted by the band-structure calculations. Another possibility for the discrepancy is electron-correlation effects, since the features in the higher-binding-energy region of the photoemission spectra reflect highly excited states where electron-correlation effects are important.

As for the Cr $3d$-derived spectrum of paramagnetic Cr_5Te_8, Fig. 12 shows that it cannot be explained by the DOS of the nonmagnetic state because the calculated DOS at the Fermi level is too high compared with the photoemission spectrum, and the ferromagnetic DOS explains the photoemission spectrum better. This may indicate the existence of short-range ferromagnetic order above the Curie temperature.[44] The calculated exchange splitting of the Cr $3d$ band, ~ 2.8 eV,[37] is two orders of magnitude larger than the Curie temperature ~ 0.03 eV,[8,9] so that the nonmagnetic state given by the band-structure calculations without spin polarization would not be realized at room temperature. The situation is the same as in Fe (Ref. 45) and Ni (Ref. 46) metals, whose spin-integrated photoemission spectra show little change between room temperature and above the Curie temperature, and are well described by the ferromagnetic DOS rather than the nonmagnetic one even above T_C.

Coulomb interaction between the Cr $3d$ electrons can be examined by comparison between the Cr $M_{2,3}VV$ Auger-electron spectra and the self-convolution of the Cr $3d$-derived spectra.[47–50] If there were no Coulomb interaction between the Cr $3d$ electrons, the $M_{2,3}VV$ Auger-electron spectra would be reproduced by the self-convolution of the Cr $3d$-derived spectra.[48,49] As shown in Fig. 13, the experimental Auger spectra of $Cr_{0.95}Te$ and Cr_5Te_8 are deformed and shifted toward lower kinetic energies compared to the self-convolutions, indicating the importance of the Coulomb interaction.[50] The intra-atomic d-d Coulomb energy (U) roughly estimated from the shift is ~ 2 eV. It is not obvious, however, whether the values of the Coulomb interaction thus determined is that between electrons of pure Cr d character or that between electrons in d orbitals hybridized with Te p orbitals. This should be examined with explicit calculations of the Auger spectra using, e.g., the cluster model. The

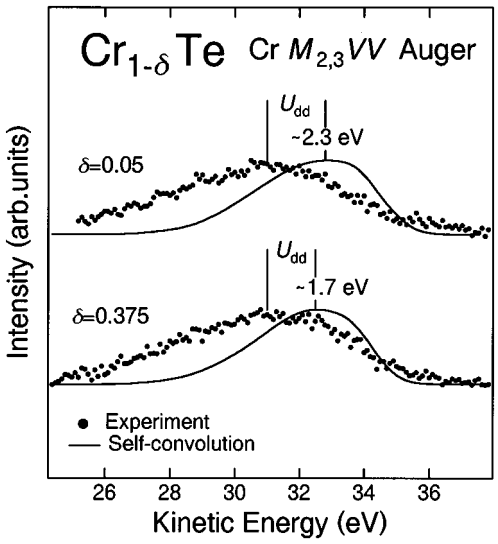

FIG. 13. Cr $M_{2,3}VV$ Auger-electron spectra of $Cr_{0.95}Te$ and Cr_5Te_8 (dots) compared with the self-convolution of the Cr $3d$-derived photoemission spectra (solid curves).

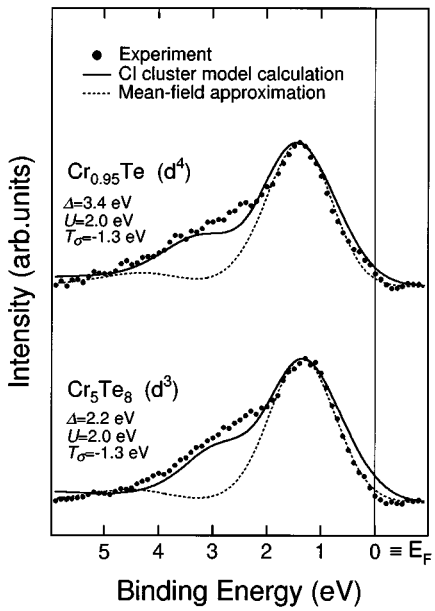

FIG. 14. Cr $3d$-derived photoemission spectra of $Cr_{0.95}Te$ and Cr_5Te_8 (dots) compared with spectra calculated using the $CrTe_6$ cluster model corresponding to the formal valences Cr^{2+} (d^4) and Cr^{3+} (d^3), respectively (solid curves). Dashed curves are given by the cluster-model calculations in the mean-field approximation.

d-band-width (W) of CrTe given by the nonmagnetic band-structure calculation is $\sim$4.6 eV,[37] which gives the ratio $U/W\sim 0.4$. Although the Coulomb interaction in $Cr_{1-\delta}Te$ is not strong compared with those in late transition-metal compounds, it is certainly not negligible.

C. Cluster-model analyses

In order to clarify electron-correlation effects and to evaluate characteristic parameters which describe the electronic states of $Cr_{1-\delta}Te$, we have performed configuration-interaction (CI) calculations on a $CrTe_6$ cluster model.[51,52] Although the system is itinerant, the model, which is based on a localized electron model, would provide us with insight into electron-correlation effects, particularly those associated with high-energy excited states as observed in the high-binding-energy region of the photoemission spectra.

The model has three adjustable parameters—the charge-transfer energy Δ, the d-d Coulomb energy U, and the transfer integral T_σ [$\equiv -\sqrt{3}(pd\sigma)$]—which are to be determined so that the calculated photoemission spectrum gives the best fit to the measured one. The relationship $(pd\sigma)/(pd\pi)\approx -2.2$ (Ref. 53) has been assumed as usual. As for the Coulomb interaction, only the diagonal term is retained. Kanamori's parameters u, u', and j (Ref. 52) have been used instead of Racah parameters A, B, and C. The Racah parameters B and C determined for the Cr ion (Table I),[54] and hence $u-u'\equiv 2j=5B+2C$, were fixed in the calculations. [Note that $U=u'-2/9j$ (Ref. 52).]

For $Cr_{0.95}Te$, we have assumed a nominal d^4 configuration, that is, the $[CrTe_6]^{10-}$ cluster model was employed. Since the total spin has to be fixed in the calculation, we have assumed the high-spin state ($S=2$). Figure 14 shows the results of the calculation. The overall features of the experimental spectrum including the high intensity at $E_B\sim 2-4$ eV have been well reproduced using $U\cong 2.0$ eV and $\Delta\cong 3.4$ eV. Obtained parameters are listed in Table II. The high-binding-energy part $E_B\sim 2-4$ eV is dominated by charge-transfer states $d^4\underline{L}$ and $d^5\underline{L}^2$ in the final state of photoemission, where $\underline{L}$ denotes a hole in the ligand Te $5p$ orbital. The value $U\cong 2.0$ eV is consistent with the result of the Auger-electron study and gives the ratio $U/W\sim 0.5$. The magnetic moment calculated from the cluster model using the above parameters is $\sim 4.1\mu_B$, which is larger than the values given by the band-structure calculations $2.4-3.5\mu_B$ (Refs. 37 and 38) and the observed saturation magnetic moment $\sim 2.5\mu_B$. In the cluster-model calculation, most electrons transferred from the ligands to the Cr ion through d-p hybridization occupy the Cr $3d$-$e_{g\uparrow}$ level, and increase the magnetic moment from the ionic value of $4\mu_B$.

In the cluster-model calculations, electron correlation within the $[CrTe_6]^{10-}$ cluster is taken into account, while in the band-structure calculations electron-electron interaction

TABLE I. Racah parameters used in the present calculations taken from Ref. 54 (in units of eV).

	B	C
Cr^{2+} (d^4)	0.100	0.442
Cr^{3+} (d^3)	0.114	0.512

TABLE II. Parameters obtained from analyses of the photoemission spectra using the CI cluster model.

	Δ (eV)	U (eV)	T_σ (eV)	n_d
$Cr_{0.95}Te$	3.4	2.0	1.3	4.4
Cr_5Te_8	2.2	2.0	1.3	3.8

is treated within the mean-field approximation. In order to clarify the relation between the CI cluster-model calculation and the band-structure calculations, we have performed cluster-model calculations in the mean-field approximation, i.e., molecular-orbital calculations without CI. That is, we have calculated the spectra replacing U by $U_{\rm MF}=0$ eV and Δ by $\Delta_{\rm MF}=\Delta+(n_d\text{-}4)U=4.2$ eV, where n_d stands for the net d-electron number ($n_d\sim4.4$ for $Cr_{0.95}Te$; see Table II). n_d is larger than the nominal number of d electrons, 4, due to charge transfer from Te $5p$ to Cr $3d$ through the p-d hybridization. As shown in Fig. 14, the spectral intensity at $E_B\sim2-4$ eV is reduced compared with the CI calculation, and the calculated spectrum generally resembles the DOS of the fully polarized state calculated by Dijkstra *et al.*[37] and Ishida and Asano.[38] Because of the large bandwidth W compared to U, and the itinerancy of electrons in this system, the use of the cluster model may not be fully justified. Indeed, detailed line shapes of the spectra could not be reproduced by cluster-model calculations. Nevertheless, the success of cluster-model calculations in reproducing the gross spectral weight distribution, especially the intensity at $E_B\sim2-4$ eV, which cannot be explained by the band-structure calculations or by the mean-field cluster calculation, demonstrates the usefulness of the cluster-model calculation to study electron-correlation effects.

The above result for $Cr_{0.95}Te$ indicates that $U<\Delta$, and locates the compound in the Mott-Hubbard-type d-band metal region of the Zeeman-Sawatzky-Allen diagram.[55] Since U and Δ are very close to each other, the p-d hybridization is large in the photoemission final state. Therefore the Te $5p$ states are also important near the Fermi level. In the ground state, the weight of the d^4 states is $\sim64\%$, while that of the $d^5\underline{L}$ state is $\sim33\%$. The first ionization states is also a strong mixture of the d^3 and $d^4\underline{L}$ states; even in the leading peak at $E_B\sim1$ eV, the contribution from the charge-transfer state is large. This is consistent with the strongly hybridized d-p bands, and shows the importance of Te $5p$ band at E_F as obtained by band-structure calculations.[37,38]

The cluster-model analysis of Cr_2O_3 (Ref. 56) has given the parameters $U=5.2$ eV and $\Delta=5.2$ eV. It is known that if we change the anions from O to Te, U and Δ decrease systematically.[57,58] The decrease in U in going from Cr_2O_3 to $Cr_{1-\delta}Te$ is, however, somewhat too large compared to what would be expected from the systematic changes found for insulating compounds.[57,58] It is possibly due to the itinerancy of the d electrons in $Cr_{1-\delta}Te$.

As for Cr_5Te_8, we have assumed a nominal d^3 high-spin configuration, and have obtained the best cluster-model fit to the experimental spectrum using $U=2.0$ eV and $\Delta\cong2.2$ eV, as shown in Fig. 14. The difference between U and Δ is smaller than that in $Cr_{0.95}Te$, locating the compound closer to the boundary between the d-band metal (Mott-Hubbard) and p-band metal (charge-transfer) regions. This is considered to be due to the higher valency of the Cr ions in Cr_5Te_8 than those in $Cr_{0.95}Te$, since Δ is known to decrease with increasing valency.[52] The net d-electron number is calculated to be $n_d\sim3.8$ (Table II), which is considerably larger than 3 due to the strong p-d hybridization. The magnetic moment calculated using the cluster model is $\sim3.4\mu_B$, which is relatively close to the band-structure calculation $3.03\mu_B$ ($\delta=0.333$) but is significantly larger than the value determined from the saturation magnetization ($<2\mu_B$). In the ground state, the weight of the $d^4\underline{L}$ state ($\sim50\%$) is larger than that of the d^3 state ($\sim37\%$) due to the strong p-d hybridization. We have also calculated the spectrum in the mean-field approximation, as shown in Fig. 14. The figure shows that in the mean-field calculation the spectral density at $E_B=2-4$ eV is again reduced, and the spectrum becomes closer to the DOS given by the band-structure calculations with full spin polarization. Therefore we conclude that electron correlation is important in giving the large spectral weight at $E_B\cong2-4$ eV in the photoemission spectra.

V. CONCLUSION

The valence-band photoemission spectra of $Cr_{0.95}Te$ ($\delta=0.05$), Cr_3Te_4 ($\delta=0.25$), and Cr_5Te_8 ($\delta=0.375$) are compared with the DOS given by the band-structure calculations[37,38] and the spectra calculated using the CI cluster model. While the overall features of the photoemission spectra agree well with the calculated DOS, some discrepancies are found: The leading peak due to the Cr $3d$-$t_{2g\uparrow}$ band in $Cr_{0.95}Te$ is shifted toward higher binding energies compared with the band-structure calculations. The photoemission intensity at the Fermi level is lower than the calculated DOS for $\delta=0.05$ and 0.375, whereas the intensity agrees well with the calculated DOS for $\delta=0.25$. The latter observation is consistent with the weakness of the electron-correlation effect in Cr_3Te_4 as suggested by the heat-capacity measurement.[39] The discrepancy between the photoemission spectra and the band-structure calculations for the peak position of the Cr $3d$-$t_{2g\uparrow}$ band in $Cr_{0.95}Te$ could not be eliminated within the collinear spin alignment if the experimental saturation magnetization is reproduced by the band-structure calculations. This may imply that $Cr_{0.95}Te$ has a noncollinear spin structure. For all δ's, the photoemission intensity at $E_B=2-4$ eV is higher than that predicted by the band-structure calculations. The photoemission spectrum of Cr_5Te_8 does not change its shape above and below the Curie temperature, and the nonmagnetic calculation cannot explain the photoemission spectra above the Curie temperature, suggesting the existence of short-range ferromagnetic order above the Curie temperature.

d-d Coulomb energies within the Cr $3d$ bands of $Cr_{0.95}Te$ and Cr_5Te_8 are estimated to be $U\sim2$ eV from the Auger-electron spectra. These values are rather small compared with the Cr $3d$ one-electron bandwidth of ~4.6 eV, but are not negligible. Indeed, the CI cluster-model calculations could explain the overall photoemission spectra, including structures in the high-binding-energy region ($E_B\sim2-4$ eV) which cannot be explained by the band-structure calculations. From cluster-model analyses, $U=2.0$ eV and $\Delta=3.4$ eV have been obtained for $Cr_{0.95}Te$, and $U=2.0$ eV and $\Delta=2.2$ eV for Cr_5Te_8. Both compounds are therefore in the d-band metal region of the Zaanen-Sawatzky-Allen diagram, but U and Δ are close to each other, particularly for Cr_5Te_8. In spite of the itinerancy of the d electrons in these compounds, the cluster model turns out to be useful to understand the gross spectral weight dis-

tribution and to obtain information about electron-correlation effects on a high-energy scale.

In order to obtain more insight into the electronic structure and electron-correlation effects in the $Cr_{1-\delta}Te$ system, information on the empty electronic states studied by inverse-photoemission spectroscopy as well as spin-dependent electronic states as probed by spin-polarized photoemission spectroscopy would be quite valuable. On the theoretical side, band-structure calculations on spin-canted structures are desirable.

ACKNOWLEDGMENTS

We would like to thank the staffs of Synchrotron Radiation Laboratory for technical support, and K. Hatakeyama for his information about the sample preparation and the crystallographic and magnetic properties of Cr_5Te_8. All calculations were performed on a VAX/VMS computer in Meson Science Laboratory, University of Tokyo. This work was supported by a Grant-in-Aid for Scientific Research from the Ministry of Education, Science and Culture, Japan.

*Present address: Department of Materials Science, Faculty of Science, Hiroshima University, Higashi-Hiroshima 724, Japan.

[1] H. H. Haraldsen and A. Neuber, Z. Anorg. Allg. Chem. **234**, 353 (1937).

[2] M. Chevreton, E. F. Bertaut, and F. Jellinek, Acta Crystallogr. **16**, 431 (1963).

[3] H. Ipser and K. L. Komarek, J. Less-Common Metals **92**, 265 (1983).

[4] N. P. Grazhdankina, L. G. Gaidukov, K. P. Rodionov, M. I. Oleinik, and A. Shchipanov, Zh. Éksp. Teor. Fiz. **40**, 433 (1961) [Sov. Phys. JETP **13**, 297 (1961)].

[5] N. P. Grazhdankina, L. A. Matyushenko, and Y. S. Bersenev, Fiz. Tverd. Tela (Leningrad) **10**, 670 (1969) [Sov. Phys. Solid State **10**, 527 (1968)].

[6] H. Ido, T. Kaneko, and K. Kamigaki, J. Phys. Soc. Jpn. **22**, 1418 (1967).

[7] A. A. Galkin, Z. A. Avadskii, and B. Ya. Sinel'nikov, Fiz. Tverd. Tela (Leningrad) **14**, 157 (1972) [Sov. Phys. Solid State **14**, 125 (1972)].

[8] K. Hatakeyama, T. Kaneko, H. Yoshida, S. Ohta, and S. Anzai, J. Magn. Magn. Mater. **90&91**, 175 (1990).

[9] S. Ohta, T. Kanomata, T. Kaneko, and H. Yoshida, J. Phys. Condens. Matter **5**, 2759 (1993).

[10] H. Ido, K. Shirakawa, T. Suzuki, and T. Kaneko, J. Phys. Soc. Jpn. **26**, 663 (1969).

[11] S. Ohta, Y. Adachi, T. Kaneko, M. Yuzuri, and H. Yoshida, J. Phys. Soc. Jpn. **63**, 2225 (1994).

[12] V. A. Gordienko, V. V. Zubenko, and V. I. Nikolaev, Zh. Éksp. Teor. Fiz. **57**, 1597 (1969) [Sov. Phys. JETP **30**, 864 (1970)].

[13] I. Tsubokawa, J. Phys. Soc. Jpn. **11**, 662 (1956).

[14] F. K. Lotgering and E. W. Gorter, J. Phys. Chem. Solids **2**, 238 (1957).

[15] L. G. Gaidukov, N. P. Grazhdankina, and I. G. Fakidov, Zh. Éksp. Teor. Fiz. **39**, 917 (1960) [Sov. Phys. JETP **12**, 636 (1961)].

[16] N. P. Grazhdankina and R. I. Zainullina, Zh. Éksp. Teor. Fiz. **59**, 1896 (1970) [Sov. Phys. JETP **32**, 1025 (1971)].

[17] A. Ohsawa, Y. Yamaguchi, N. Kazama, H. Yamaguchi, and H. Watanabe, J. Phys. Soc. Jpn. **33**, 1303 (1972).

[18] T. Hirone and S. Chiba, J. Phys. Soc. Jpn. **15**, 1991 (1960).

[19] T. Hashimoto and M. Yamaguchi, J. Phys. Soc. Jpn. **27**, 1121 (1969).

[20] S. Ohta, S. Kurosawa, and S. Anzai, J. Phys. Soc. Jpn. **51**, 1386 (1981).

[21] T. Hashimoto and M. Yamaguchi, J. Phys. Soc. Jpn. **27**, 1121 (1969).

[22] M. Yamaguchi and T. Hashimoto, J. Phys. Soc. Jpn. **32**, 635 (1972).

[23] S. Ohta, A. Fujii, and S. Anzai, J. Phys. Soc. Jpn. **52**, 1765 (1983).

[24] S. Ohta, J. Phys. Soc. Jpn. **54**, 1076 (1985).

[25] Y. Sugimoto, S. Ohta, S. Yuri, M. Tamaki, and S. Anzai, J. Phys. Soc. Jpn. **54**, 3240 (1985).

[26] T. Hashimoto, K. Hoya, M. Yamaguchi, and I. Ishitsubo, J. Phys. Soc. Jpn. **31**, 679 (1971).

[27] K. Hatakeyama, S. Anzai, S. Ohta, H. Yoshida, and T. Kaneko (unpublished).

[28] C. Guillaud and S. Barbezat, C. R. Acad. Sci. **222**, 386 (1946); C. Guillaud, *ibid.* **222**, 1224 (1946).

[29] A. F. Andresen, Acta Chem. Scand. **24**, 3495 (1970).

[30] T. Hamasaki, T. Hashimoto, Y. Yamaguchi, and H. Watanabe, Solid State Commun. **16**, 895 (1975).

[31] A. F. Andresen, Acta Chem. Scand. **17**, 1335 (1963).

[32] E. F. Bertaut, G. Roult, R. Aleonard, R. Pauthenet, M. Chevreton, and R. Jansen, J. Phys. (Paris) **25**, 582 (1964).

[33] D. E. Cox, G. Shirane, and W. J. Takei, in *Proceedings of the International Conference on Magnetism, Nottingham, 1964*, edited by A. C. Stickland (Institute of Physics and the Physical Society, London, 1965), p. 291.

[34] W. J. Takei, D. E. Cox, and G. Shirane, J. Appl. Phys. **37**, 973 (1966).

[35] B. Lambert-Andron, N. P. Grazhdankina, and C. Vettier, J. Phys. (Paris) **39**, L43 (1978).

[36] B. B. Starichenko and A. N. Pigorov, Fiz. Met. Ikh Soedin. **1979**, 56.

[37] J. Dijkstra, H. H. Weitering, C. F. van Bruggen, C. Haas, and R. A. de Groot, J. Phys. Condens. Matter **1**, 9141 (1989).

[38] S. Ishida and S. Asano (unpublished).

[39] F. Grønvold and E. F. Westrum, Jr., Z. Anorg. Allg. Chem. **328**, 272 (1964).

[40] K. Sato, Y. Aman, M. Hirai, and M. Fujisawa, J. Phys. Soc. Jpn. **59**, 435 (1990); K. Sato, Y. Aman, and M. Hirai, J. Phys. (Paris) Colloq. **49**, C8-213 (1988).

[41] J. J. Yeh and I. Lindau, At. Data Nucl. Data Tables **32**, 1 (1985).

[42] J. F. van Acker, Z. M. Standnik, J. C. Fuggle, H. J. W. M. Hoekstra, K. H. J. Buschow, and G. Sroink, Phys. Rev. B **37**, 6827 (1988).

[43] D. A. Shirley, in *Photoemission in Solids I*, edited by M. Cardona and L. Ley (Springer-Verlag, Heidelberg, 1978), Chap. 4, p. 165.

[44] R. E. Prange and V. Korenman, Phys. Rev. B **19**, 4691 (1979).

[45] E. Kisker, K. Shröder, W. Gudat, and M. Campagna, Phys. Rev. B **31**, 329 (1985).

[46] H. Hopster, R. Raue, E. Kisker, G. Güntherodt, and M. Campagna, Phys. Rev. Lett. **50**, 329 (1983).

[47] J. J. Lander, Phys. Rev. **91**, 1382 (1953).

[48] M. Cini, Solid State Commun. **24**, 681 (1977).

[49] G. A. Sawatzky, Phys. Rev. Lett. **39**, 504 (1977).

[50] G. A. Sawatzky and A. Lenselink, Phys. Rev. B **21**, 1790 (1980).

[51] A. Fujimori and F. Minami, Phys. Rev. B **30**, 957 (1984).

[52] A. E. Bocquet, T. Mizokawa, T. Saitoh, H. Namatame, and A. Fujimori, Phys. Rev. B **46**, 3771 (1992); A. E. Bocquet, T. Saitoh, T. Mizokawa, and A. Fujimori, Solid State Commun. **83**, 11 (1992); T. Saitoh, A. E. Bocquet, T. Mizokawa, H. Namatame, A. Fujimori, M. Abbate, Y. Takeda, and M. Takano, Phys. Rev. B **51**, 13 942 (1995).

[53] W. A. Harrison, *Electronic Structure and the Physical Properties of Solids* (Dover, New York, 1989).

[54] Y. Tanabe and S. Sugano, J. Phys. Soc. Jpn. **9**, 766 (1954).

[55] J. Zaanen, G. A. Sawatzky, and J. W. Allen, Phys. Rev. Lett. **55**, 418 (1985).

[56] X. Li, V. E. Henrich, T. Saitoh, and A. Fujimori, in *Applications of Synchrotron Radiation Techniques to Materials Science*, edited by D. L. Perry, N. Shinn, R. Stockbauer, K. D'Amico, and L. Terminello, MRS Symposia Proceedings No. 307 (Materials Research Society, Pittsburgh, 1993), p. 205.

[57] A. Fujimori, A. E. Bocquet, T. Saitoh, and T. Mizokawa, J. Electron Spectrosc. Relat. Phenom. **62**, 141 (1993).

[58] T. Mizokawa and A. Fujimori, Phys. Rev. B **48**, 14 150 (1993).